

Collective and Independent-Particle Motion in Two-Electron Artificial Atoms

Constantine Yannouleas and Uzi Landman

School of Physics, Georgia Institute of Technology, Atlanta, Georgia 30332-0430

(Received 14 March 2000)

Investigations of the exactly solvable excitation spectra of two-electron quantum dots with a parabolic confinement, for different values of the parameter R_W expressing the relative magnitudes of the interelectron repulsion and the zero-point kinetic energy, reveal for large R_W a rovibrational spectrum associated with a linear trimeric rigid molecule composed of the two electrons and the infinitely heavy confining dot. This spectrum transforms to that of a “floppy” molecule for smaller R_W . The conditional probability distribution calculated for the exact two-electron wave functions allows identification of the rovibrational excitations as rotations and stretching/bending vibrations.

PACS numbers: 73.20.Dx, 71.45.Lr, 73.23.-b

The behavior of three-body systems has been a continuing subject of interest and a source of discoveries in various branches of physics, both in the classical and quantum regimes, with the moon-earth-sun system [1] and helium-like atoms [2–7] (in the ground and excited states) being perhaps the best known examples. Furthermore, insights gained through such investigations often provide the foundations for understanding the properties of systems with a larger number of interacting particles.

Recently, analysis of the measured conductance [8] and differential capacitance [9] spectra of two-dimensional (2D) quantum dots (QD's), created via voltage gates at semiconductor heterointerfaces, led to their naming (by analogy) as “artificial atoms.” In particular, this analogy refers to identification of regularities in the measurements which have been interpreted [8] along the lines of the electronic shell model of natural atoms, which is founded on the physical picture of electrons moving in a *spherical central* field including the averaged contribution from electron-electron interactions.

Motivated by the central role that spectroscopy played in the development of our understanding of atomic structure, we investigate in this paper the exactly solvable excitation spectrum of a two-electron (2e) parabolic QD as a prototypical three-body problem comprised of the two electrons (X 's) and the (infinitely heavy) confining quantum dot (Y). Through probing of the structure of the exact wave functions with the use of the conditional probability distribution (CPD) [3], in conjunction with identification of regularities of the excitation spectrum, we show that such a spectrum is characteristic of collective dynamics resulting from formation of a linear trimeric molecule XYX [10]. In particular, we find that the excitation spectrum of the 2e QD exhibits for a weak parabolic confinement (i.e., small harmonic frequency ω_0) a well-developed, separable rovibrational pattern which is akin to the characteristic spectrum of natural “rigid” triatomic molecules (i.e., molecules with stretching and bending vibrational frequencies higher than the rotational one). For stronger confinements (i.e., large ω_0), the spectrum transforms to one characteristic of a “floppy” triatomic molecule, converging finally to the independent-

particle picture associated with the circular central mean field of the QD.

The Schrödinger equation for a 2e QD with a parabolic confinement of frequency ω_0 , with the 2D Hamiltonian given by $H = \sum_{i=1,2} \mathbf{p}_i^2/2m^* + e^2/\kappa|\mathbf{r}_1 - \mathbf{r}_2| + 0.5m^*\omega_0^2 \sum_{i=1,2} \mathbf{r}_i^2$, where κ and m^* are, respectively, the dielectric constant and electron effective mass, is separable in the center-of-mass (c.m.) and relative-motion (rm) coordinates [11]. Consequently, the energy eigenvalues may be written as $E_{NM, nm} = E_{NM}^{c.m.} + \varepsilon^{rm}(n, |m|)$, where $E_{NM}^{c.m.} = \hbar\omega_0(2N + |M| + 1)$ with the N and M quantum numbers corresponding to the number of radial nodes in the c.m. wave function and M is the c.m. azimuthal quantum number; $\varepsilon^{rm}(n, |m|)$ are the eigenvalues of the one-dimensional Schrödinger equation [11],

$$\frac{\partial^2 \Omega}{\partial u^2} + \left\{ \frac{-m^2 + 1/4}{u^2} - u^2 - \frac{R_W \sqrt{2}}{u} + \frac{\varepsilon}{\hbar\omega_0/2} \right\} \Omega = 0,$$

where $\Omega(u)/\sqrt{u}$ is the radial part of the rm wave function $\Omega(u)e^{im\theta}/\sqrt{u}$ with n being the number of radial nodes; $u = |\mathbf{u}_1 - \mathbf{u}_2|$ with $\mathbf{u}_i = \mathbf{r}_i/l_0\sqrt{2}$ ($i = 1, 2$) being the electrons' coordinates in dimensionless units and $l_0 = (\hbar/m^*\omega_0)^{1/2}$, that is the spatial extent of the lowest-state wave function of a single electron. The so-called Wigner parameter $R_W = (e^2/\kappa l_0)/\hbar\omega_0$ multiplying the Coulomb repulsion term expresses the relative strength of the Coulomb repulsion between two electrons separated by l_0 and twice the zero-point kinetic energy of an electron moving in a harmonic confinement.

Denoting the exact spatial wave function of the 2e QD by $\Phi_{NM, nm}(\mathbf{u}_1, \mathbf{u}_2)$ (which is the product of the c.m. and rm wave functions), and the spatial two-electron density by $W_{NM, nm}(\mathbf{u}_1, \mathbf{u}_2) = |\Phi_{NM, nm}(\mathbf{u}_1, \mathbf{u}_2)|^2$, we define the usual pair-correlation function (PCF) as

$$G(\mathbf{v}) = 2\pi \int \int \delta(\mathbf{u}_1 - \mathbf{u}_2 - \mathbf{v}) W(\mathbf{u}_1, \mathbf{u}_2) d\mathbf{u}_1 d\mathbf{u}_2,$$

and the CPD for finding one electron at \mathbf{v} given that the other is at \mathbf{v}_0 as

$$\mathcal{P}(\mathbf{v} | \mathbf{u}_2 = \mathbf{v}_0) = \frac{W(\mathbf{v}, \mathbf{u}_2 = \mathbf{v}_0)}{\int d\mathbf{u}_1 W(\mathbf{u}_1, \mathbf{u}_2 = \mathbf{v}_0)},$$

where the M , N , n , and m indices of W (and therefore of G and \mathcal{P}) have been suppressed. Note that the exact electron densities are circularly symmetric.

With the above, we solved for the $2e$ QD energy spectra and wave functions for values of $R_W = 200, 20$, and 3 . We discuss first the $R_W = 200$ case whose spectrum and selected PCF's and CPD's are displayed in Fig. 1. As can be seen immediately, for such a large value of R_W , the spectrum of the $2e$ QD (bottom part of Fig. 1) exhibits the following three well-developed regularities: (I) for

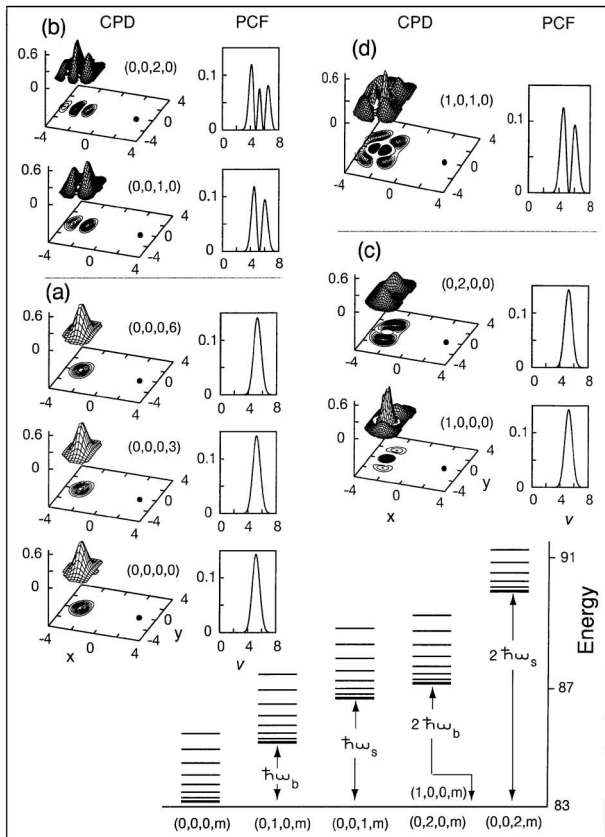


FIG. 1. Spectra (bottom) and corresponding conditional probability distributions (CPD's) and pair-correlation functions (PCF's) shown, respectively, on the left and right of each of the subplots [labeled (a)–(d)], for a $2e$ QD with $R_W = 200$. For each excitation band, the quantum numbers (N_0, M_0, n_0, m) are given at the bottom with $m = 0, 1, 2, \dots$ (the levels for $m = 0$ and $m = 1$ are not resolved on the scale of the figure and appear as a thick line); only a few of the low lying rotational and vibrational states are shown, with the collective rovibrational behavior extending to higher excitations. The CPD's and PCF's are labeled with the quantum numbers of the corresponding levels. For the spectral rules governing the spectrum and for the definition and interpretation of the CPD's and PCF's, see the text. The solid dot in each of the CPD subplots denotes the point $\mathbf{v}_0 = (d_0, 0)$, where $d_0 = 2.6$ is half of the electron separation found in the PCF of the ground state $(0, 0, 0, 0)$. All distances x , y , v , and d_0 are in units of $l_0\sqrt{2}$, and energies are in units of $\hbar\omega_0/2$.

every band (N_0, M_0, n_0, m) , with $m = 0, 1, 2, \dots$, while N_0 , M_0 , and n_0 are kept constant (in the following the subscript “zero” denotes a number that is held constant in a particular sequence), the energy spacing between two adjacent levels m and $m + 1$ increases linearly in proportion to $2m + 1$; the bands $(N_0, \pm M_0, n_0, \pm m)$ are degenerate. Note that the levels are spin singlet or triplet for m even or odd, respectively, (II) the bands $(0, M_0, 0, m)$ and $(N_0, 0, 0, m)$ correspond to excitations of the center-of-mass motion with M_0 and $2N_0$ vibrational quanta (phonons) of energy $\hbar\omega_0$, respectively, and (III) the bottom levels of the bands $(0, 0, n_0, m)$ form a one-dimensional harmonic-oscillator spectrum $(n_0 + 1/2)\hbar\omega_s$.

The above three “spectral rules” specify a well-developed and separable rovibrational spectrum exhibiting collective rotations, as well as stretching and bending vibrations [12]. Indeed, neglecting an overall constant term, the above rules can be summarized as

$$E_{NM, nm} = Cm^2 + (n + 1/2)\hbar\omega_s + (2N + |M| + 1)\hbar\omega_b,$$

where the rotational constant $C \approx 0.037$, the phonon for the stretching vibration has an energy $\hbar\omega_s \approx 3.50$, and the phonon for the bending vibration coincides with that of the c.m. motion, i.e., $\hbar\omega_b = \hbar\omega_0 = 2$ [12,13] (all energies are given in dimensionless units of $\hbar\omega_0/2$). Note that the rotational energy is proportional to m^2 , as is appropriate for 2D rotations, unlike the case of natural triatomic molecules where the rotational energy has a term proportional to $l(l + 1)$, l being the quantum number associated with the 3D angular momentum. Observe also that the bending vibration can carry by itself an angular momentum $\hbar M$ and thus the rotational angular momentum $\hbar m$ does not necessarily coincide with the total angular momentum $\hbar(M + m)$.

Further insight into the collective character of the spectrum displayed in Fig. 1 can be gained by examining the CPD's and PCF's associated with selected states of the rotational bands (N_0, M_0, n_0, m) (the CPD's are displayed to the left of the PCF's; notice that the PCF's are always circularly symmetric). The band $(0, 0, 0, m)$, being *purely* rotational with zero phonon excitations, can be designated as the “yrast” band, in analogy with the customary terminology from the spectroscopy of rotating nuclei [14].

In Fig. 1(a), we display the CPD's and PCF's for three specific states of the yrast band, i.e., the $(0, 0, 0, 0)$, the $(0, 0, 0, 3)$, and the $(0, 0, 0, 6)$. The corresponding PCF's are all alike and centered around $2d_0 = 5.2$, which implies that the two electrons keep apart from each other at a distance $2d_0$. Because of the circular symmetry of the PCF's, however, one can conclude only that the two electrons are moving on a thin circular shell of radius d_0 . To reveal the formation of an electron molecule, one needs to consider further the corresponding CPD's [plotted in the left column with $\mathbf{v}_0 = (d_0, 0)$; the point \mathbf{v}_0 is denoted by

a solid dot]. In fact, the CPD's demonstrate that the two electrons reside at all instances at diametrically opposite points, thus forming a linear molecule XYX with two equal bonds ($X-Y$ and $Y-X$) of length d_0 . In addition, one can see that all three CPD's are practically identical, in spite of the fact that the angular momentum changes from $m = 0$ (lower subplot) to $m = 6$ (upper subplot). This behavior, namely, the constancy of the bond lengths irrespective of the rotational energy, properly characterizes the electron molecule as a rigid rotor.

Turning our attention away from the yrast band, we focus next on the bands $(0, 0, 1, m)$ and $(0, 0, 2, m)$, which are rotational bands built upon one- and two-phonon excitations of the stretching vibrational mode. We have verified that the PCF's and the CPD's corresponding to these bands share with the yrast band the property that they do not change (at least for the levels displayed in Fig. 1) as a function of m . Thus it is sufficient to study the bottom states, i.e., those with $m = 0$, $(0, 0, 1, 0)$ and $(0, 0, 2, 0)$, whose corresponding PCF's and CPD's are displayed in the lower and upper subplots of Fig. 1(b), respectively. The PCF's demonstrate the presence of internal excitations with one and two nodes in the relative motion, but they yield no further information regarding the electron molecule. The CPD's, however, plotted here for $\mathbf{v}_0 = (d_0, 0)$ (the point \mathbf{v}_0 is kept the same for all subplots in Fig. 1) immediately reveal the presence of excitations (specified by the number of their nodes, i.e., here one or two) associated with the vibrational mode of the XYX molecule *along* the interelectron axis (namely, the stretching vibration).

By examining the corresponding CPD's, one can further demonstrate that the two degenerate rotational bands $(0, 2, 0, m)$ and $(1, 0, 0, m)$ are built upon the lowest two-phonon excitations of the bending vibrational mode of the linear molecule XYX . Again, we have verified that it is sufficient to consider the two states at the bottom of the bands, namely, the $(1, 0, 0, 0)$ [see lower subplot of Fig. 1(c)] and the $(0, 2, 0, 0)$ [see upper subplot of Fig. 1(c)]. It can be seen that both CPD's describe vibrational excitations of the XYX molecule which are *perpendicular* to the interelectron axis (namely, bending vibrations), with the one associated with the $(1, 0, 0, 0)$ level having one node and the one associated with the $(0, 2, 0, 0)$ having no nodes (this is in agreement with the fact that the normal mode associated with the bending vibrations is related to the 2D harmonic oscillator describing the c.m. motion). We note that the corresponding PCF's [see right column in Fig. 1(c)] fail to describe (in fact, they are completely unrelated to) the bending vibrations; indeed they are identical to the ones associated with the yrast band [Fig. 1(a)] which is devoid of any vibrational excitations.

The CPD and PCF of the bottom level (i.e., with $m = 0$) of the rotational band $(1, 0, 1, m)$, which is built upon more complicated phonon excitations of mixed bending and stretching character (not shown in Fig. 1), are displayed in Fig. 1(d). It is easily seen that the CPD represents a

vibrational motion of the electron molecule both along the interelectron axis (one excited stretching-mode phonon) and perpendicularly to this axis (two excited bending-mode phonons). In fact, the CPD in Fig. 1(d) can be viewed as a composite made out of two CPD's shown previously, one in the lower subplot of Fig. 1(b) and the other in the lower subplot of Fig. 1(c). Returning to Fig. 1(d), one can see again that, in contrast to the CPD which enables detailed probing of the excitation spectrum, the information which may be extracted from the corresponding PCF is rather limited.

The rigidity of the electron molecule, which is so well established for $R_W = 200$, will naturally weaken as the parameter R_W decreases and the XYX molecule will start exhibiting an increasing degree of "floppiness." Such floppiness can be best observed in the yrast band, which, beginning with the higher levels, will gradually deviate from the spectral rule (I) discussed above, and eventually it will become unrecognizable as a rotational band. This is illustrated in the lower subplot of Fig. 2(a) which displays the yrast band for $R_W = 20$. Specifically, one can see that

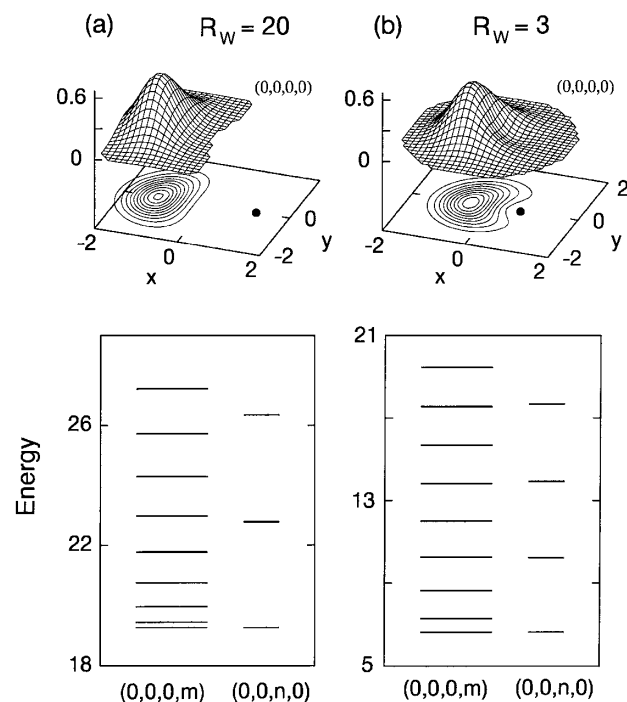


FIG. 2. Spectra (bottom) and CPD's (top) of the corresponding ground-state levels for 2e QD's with (a) $R_W = 20$, and (b) $R_W = 3$. At each of the bottom panels, the spectrum of the yrast band [i.e., $(0, 0, 0, m)$; $m = 0, 1, 2, \dots$] is shown on the left, and the lowest levels of the bands $(0, 0, n_0, m)$ for $n_0 = 0, 1, 2, \dots$, forming a stretching vibrational spectrum (i.e., with constant spacing) are displayed on the right. The solid dot in each of the CPD subplots denotes the point $\mathbf{v}_0 = (d_0, 0)$, where d_0 is half of the electron separation found in the corresponding ground-state PCF's (not shown here). Energies in units of $\hbar\omega_0/2$ and distances in units of $l_0\sqrt{2}$; e.g., for GaAs material parameters ($m^* = 0.067m_e$, $\kappa = 12.9$) and $R_W = 3$, one has $\hbar\omega_0 = 1.2$ meV and $l_0\sqrt{2} = 43.54$ nm.

only the lowest four levels honor approximately rule (I), the higher ones tending to develop a constant energy spacing between adjacent levels [this spacing converges slowly to the energy spacing $\hbar\omega_0$ (i.e., to the value 2 in dimensionless units) of the parabolic confinement]. In the case $R_W = 3$, one can hardly identify any rotational sequence in the levels of the yrast band [plotted at the bottom subplot of Fig. 2(b)]. Indeed, although the energy spacing between the second and the third levels is larger than that between the first and the second levels (but with a ratio substantially different than 3/1), the spacing between higher levels approaches quickly the value 2 of the external confinement.

However, in spite of the floppiness exhibited by the excitation spectra in Fig. 2, the (singlet) ground state of the 2e QD for both $R_W = 20$ and $R_W = 3$ drastically deviates from the $1s^2$ close-shell orbital configuration expected from the independent-particle picture. Rather, as demonstrated by the corresponding CPD's (top subplots in Fig. 2), in both these cases of smaller R_W 's, the ground state is still associated with formation of rather well-developed *XYX* electron molecules, but with progressively smaller bond lengths. Finally, we remark that the stretching vibrations are more robust and tend to better preserve a constant spacing between the bottom levels of the bands $(0, 0, n_0, m)$ [these levels were grouped in a vibrational band $(0, 0, n, 0)$ and are plotted on the right-hand side of the lower subplots in Fig. 2].

The remarkable emergence of rovibrational excitations for parabolically confined 2e QD's, under magnetic-field-free conditions, provides direct evidence for the formation of electron molecules in QD's, with their rigidity controlled by the parameter R_W . Such electron molecules and associated collective excitation spectra are general properties [15–17] of QD's (with greater spectral complexity in many-electron QD's), whose observations (and manipulations through controlled pinning of the collective rotations [15(b)]) form outstanding experimental challenges.

This research is supported by the U.S. D.O.E. (Grant No. FG05-86ER-45234).

-
- [1] M. C. Gutzwiller, *Rev. Mod. Phys.* **70**, 589 (1998).
 [2] (a) M. E. Kellman and D. R. Herrick, *J. Phys. B* **11**, L755 (1978); (b) *Phys. Rev. A* **22**, 1536 (1980); (c) see also the comprehensive review by M. E. Kellman, *Int. J. Quantum Chem.* **65**, 399 (1997).
 [3] H.-J. Yuh *et al.*, *Phys. Rev. Lett.* **47**, 497 (1981); G. S. Ezra and R. S. Berry, *Phys. Rev. A* **28**, 1974 (1983); see also the review by R. S. Berry, *Contemp. Phys.* **30**, 1 (1989).
 [4] J. M. Rost *et al.*, *J. Phys. B* **24**, 2455 (1991); J. M. Rost and J. S. Briggs, *ibid.* **24**, 4293 (1991).
 [5] D. Wintgen, K. Richter, and G. Tanner, *Chaos* **2**, 19 (1992).
 [6] V. N. Ostrovsky and N. V. Prudov, *Phys. Rev. A* **51**, 1936 (1995).

- [7] See the review by C. D. Lin, *Adv. At. Mol. Phys.* **22**, 77 (1986).
 [8] S. Tarucha *et al.*, *Phys. Rev. Lett.* **77**, 3613 (1996).
 [9] R. C. Ashoori, *Nature (London)* **379**, 413 (1996).
 [10] Molecular behavior of a nonrigid linear structure undergoing collective rotation and vibration has been studied in the context of excited states of two-electron atoms (Refs. [2–7]).
 [11] R. M. G. Garcia-Castelan *et al.*, *Phys. Rev. B* **57**, 9792 (1998); U. Merkt *et al.*, *Phys. Rev. B* **43**, 7320 (1991); M. Taut, *J. Phys. A* **27**, 1045 (1994).
 [12] For the 2D 2e QD system, letting $s = r_1 + r_2$, $t = (r_1 - r_2)/2$, and defining θ_{12} to be the interelectron angle with respect to the center of the dot, the classical equilibrium point for the two antipodal electrons is $s_0^3 = 2e^2/(\kappa m^* \omega_0^2)$, $t_0 = 0$, and $\theta_{12} = \pi$. Note that, for $\theta_{12} = \pi$, s and t correspond to relative and c.m. motions along the interelectron axis. In addition, s is associated with the symmetric stretch, t with the antisymmetric stretch, and θ_{12} with the bend perpendicular to the interelectron axis. The classical potential energy (see the potential terms in the Hamiltonian given in the text), expanded around the equilibrium point (for a similar analysis for a 2e natural atom, see Ref. [2(b)]), is given by $V(s_0 + \delta s, \delta t, \delta q) = 3e^2/(2\kappa s_0) + 1.5\mu\omega_0^2\delta s^2 + 0.5\mathcal{M}\omega_0^2(\delta q^2 + \delta t^2)$, where μ is the 2e reduced mass and $\mathcal{M} = 2m^*$. $\delta q = s_0(\pi - \theta_{12})/4$, being the displacement of the c.m. of the two electrons perpendicular to the interelectron axis, is associated with the bending vibration. It is apparent that the classical symmetric stretch has a frequency of $\sqrt{3}\omega_0$. The antisymmetric stretch and the bend are degenerate with frequency ω_0 , and together they generate a two-dimensional vibration which coincides with the 2e c.m. motion and carries angular momentum. Since the CPD corresponding to this mode exhibits bendinglike behavior [see Fig. 1(c)], we refer to it as a bending mode.
 [13] To connect to the ordinary notation used in molecular spectroscopy [I. V. Levine, *Quantum Chemistry* (Allyn and Bacon, Boston, 1970), Vol. II], we note that n corresponds to ν_1 (i.e., symmetric stretch). In light of Ref. [12], $2N + |M|$ does not correspond directly to either ν_2 (bending in 3D) or ν_3 (antisymmetric stretch); note, however, that this quantum number varies in the same way as does ν_2 in the case of natural linear 3D triatomic molecules.
 [14] See, e.g., Å. Bohr and B. R. Mottelson, *Nuclear Structure* (Benjamin, Reading, MA, 1975), Vol. II, p. 41; see also Ref. [2(a)].
 [15] (a) C. Yannouleas and U. Landman, *Phys. Rev. Lett.* **82**, 5325 (1999); (b) *Phys. Rev. B* **61**, 15 895 (2000).
 [16] Formation of electron molecules in QD's has been discussed in Ref. [15] in the context of symmetry-breaking states of the self-consistent field resulting from spin-and-space unrestricted Hartree-Fock calculations.
 [17] For a discussion of excitations of electron molecules in fully polarized parabolic QD's in high magnetic fields, see also P. A. Maksym, *Phys. Rev. B* **53**, 10 871 (1996); H.-M. Müller and S. E. Koonin, *Phys. Rev. B* **54**, 14 532 (1996).